Temperature dependence of fluxoid quantization
in a superconducting hollow cylinder

H. J. Fink* and V. Grünfeld†

*Centro Atómico Bariloche, Comisión Nacional de Energía Atómica,
and Instituto Balseiro, Universidad Nacional de Cuyo, 8400 S. C. de Bariloche (R.N.), Argentina*

(Received 21 January 1980)

Using the Ginzburg-Landau theory the magnetic response of a long hollow cylinder is calculated. Emphasis is placed on the magnetic properties as a function of temperature in a constant applied magnetic field. The only restriction is that the wall thickness is less than twice the temperature-dependent coherence length. The penetration depth is of arbitrary value as are the cylinder radius and wall thickness. The fluxoid is quantized. In the limit that the order parameter approaches zero, we obtain the quasiperiodic magnetic-field-temperature phase boundary between the normal and superconducting states. This boundary is either a second-order phase transition or a supercooling boundary. The dividing point between the two, the Landau critical point, was derived and investigated for arbitrary values of the fluxoid quantum number. The latter does not always exist for arbitrary cylinder dimensions and quantum numbers. A consequence of the appearance of a supercooling boundary is a superheating boundary which was obtained numerically from the nonlinear equations. The latter may exist, in particular for larger fluxoid quantum numbers, at a temperature beyond that of the maximum supercooling temperature. Agreement of our results with published experiments is found to be good.

I. INTRODUCTION

Recent experiments[1] show that a large, solid, type-I superconducting cylinder with a surface sheath ($\kappa > 0.42$) in a constant applied axial magnetic field H_o, larger than the thermodynamic critical field $H_c(T)$, changes its magnetic moment reversibly from diamagnetic for temperatures just below $T(H_{c3})$ to paramagnetic just above $T(H_c)$ when thermally cycled. The theoretical explanation of these experiments[1] was based upon the premise that the fluxoid quantum number was conserved when thermally cycled over *large* temperature intervals and the quantum number was uniquely determined[2] when sweeping the temperature from above $T(H_{c3})$ to lower temperatures. The adiabatic invariance of the fluxoid under *small* thermal perturbations was found previously in thin-film rings.[3,4]

Experiments by Little and Parks,[5] Groff and Parks,[6] and Meyers and Meservey[7] show that the magnetic phase boundary between the normal (N) and superconducting (S) states of thin-walled microcylinders is a quasiperiodic function of temperature. This is a consequence of fluxoid conservation as suggested originally by Little and Parks[5] based upon the theory of Byers and Yang.[8] The existence of the superconducting fluxoid was established by the experiments of Deaver and Fairbank[9] and Doll and Näbauer[10] and later by Goodman et al.[11] Theoretical explanations are given by Onsager,[12] Bardeen,[13] and Keller and Zumino.[14]

Approximate equations of the quasiperiodic varia-

tion of the NS phase boundary were derived for thin-walled microcylinders with certain assumptions by Tinkham[15,16] including the angular variation of the latter when the magnetic field is tilted with respect to the axis of the cylinder. The angular variation was investigated experimentally by Meservey and Meyers.[17]

Previous to the measurements of Ref. 1 there had been evidence of fluxoid conservation effects by measuring the magnetic moment of superconducting cylinders when sweeping a magnetic field between $H_{c3}(T)$ and $H_c(T)$ at constant temperature (Refs. 18 and 19). In that case the conservation of the fluxoid quantum state was linked to the induced currents produced by the change of the external field and was evidenced by the reversibility of the magnetization upon cycling of the applied magnetic field. Exceeding the critical current causes a change in the fluxoid quantum number in a solid cylinder.[20] The sample then switches into a different quantum state and the magnetic moment does not behave any longer reversibly[18-20] when reversing the direction of the variation of the magnetic field. The explanation of these experiments[18-20] can be linked to the concept of the giant vortex[21] which was also employed in explaining the experiments of de la Cruz et al.[1]

A *singly* connected surface sheath in its lowest-energy state has two opposing currents of equal magnitude. The temperature dependence of the spatially varying current density is then responsible for the temperature-dependent magnetic properties.[1,22] On a large cylinder this state can be realized by destroying

superconductivity along a strip parallel to the axis of the sample. The superconducting surface region then becomes singly connected and the fields outside and deep inside the cylinder have the same value. This condition ensures that there is no net current in the surface sheath.[1,22] Since the order parameter is finite in the sheath, the superfluid velocity must be zero on some open contour inside the surface sheath. At this point the current density changes sign.

When the sample is *multiply* connected, the zero-current contour becomes a closed circle in the plane perpendicular to the axis of the cylinder. This new constraint forces the field inside the cylinder to adjust itself so as to keep the quantum state fixed. A consequence of this constraint is a *net* temperature-dependent current in the surface sheath, caused by an imbalance of the two opposing surface-sheath currents, which is mainly responsible for the temperature-dependent magnetic properties[1] of the multiply connected sheath. A manifestation of this constraint is also a quasiperiodic variation of the surface critical field H_{c3} with cylinder radius R.[23–25]

In the experiments of Ref. 1 the applied field was kept constant but it was found that the total flux through the sample changed when sweeping temperature. The obvious conclusion is that the closed contour of zero velocity adjusts itself with temperature in order to keep the fluxoid quantum number constant. It is important to realize that a zero magnetic moment below $T_3(H_o)$ (surface critical temperature) does not mean that H_o is equal to $H(0)$, the field in the center of the cylinder. The field $H(0)$ can be equal to H_o and the magnetic moment zero *only* for temperatures higher than T_3 or for a material with infinite penetration depth. In the latter case, no magnetic effects are observed. It is then reasonable to think, when the magnetic moment below T_3 is zero, that the field $H(0)$ is larger than H_o in order to compensate for the expulsion of the field from the surface superconducting region. Clearly one is not allowed to make the approximation of constant current density across the surface sheath as it is often done, for example, over the wall thickness of a hollow cylinder. This argument is valid, in general, independently of whether T or H_o is the external variable. In the latter instance one might conceive of an experiment in which the zero-current-density contour is driven out of the sample. This can happen only for fixed quantum states in certain temperature or field ranges, when the field $H(0)$ is very different from H_o (always within the limits imposed by the critical currents). In this case the magnetization is either strongly paramagnetic or strongly diamagnetic and the approximation of constant current density across the surface will then be very approximately valid.

We feel that the above arguments elucidate the essential physics better than the usual consideration of having a penetration depth long in comparison to the thickness of the superconducting region, since the magnetic properties tend to zero in the latter case. From the above discussion it seems that surface superconductivity or the giant-vortex state does not seem to be a necessary condition for the inversion of magnetization to be observed. We have, therefore, decided to investigate the magnetic response of a hollow cylinder in particular with emphasis on its temperature dependence in a constant applied magnetic field. The only assumptions we make are: (a) the cylinder is long enough so that demagnetization effects can be neglected, and (b) the wall thickness, d, of the cylinder is smaller than $2\xi(T)$ while the penetration depth $\lambda(T)$ is arbitrary. The latter assumption implies that the modulus of the order parameter, f, is approximately a constant over the wall thickness of the cylinder and the solutions are then valid for Ginzburg-Landau (GL) κ values smaller than $2\lambda/d$.

Within the context of the London equations Lipkin *et al.*[26] developed the general equations for the magnetic response of a hollow cylinder. These were developed further by Douglass[27] in general terms of the Ginzburg-Landau theory with the same assumptions as stated above. Douglass[27] then investigates in detail the case $\lambda(T) >> d$.

This work is also based upon the Ginzburg-Landau theory. The GL theory, which is local, can be modified to take nonlocal effects into account $[\lambda(t) < \xi_o = 0.18\hbar v_F/kT_c]$. These modifications are discussed in Ref. 28, Sec. 2.7. The general considerations in the following Sec. II up to Eq. (16) are conceptually similar to Douglass's work up to his Eq. (27). In Sec. III the limit of f approaching zero is investigated including the magnetization for $f << 1$ and the Landau critical point (LCP), the dividing point between first- and second-order NS phase transitions. Complete solutions of the nonlinear GL equations are presented in Sec. IV and in Sec. V we make comparisons of our results with published experiments. Section VI is devoted to the conclusions.

II. THEORY

Consider a hollow cylinder of wall thickness d, outside radius R, and inside radius R_o. The applied magnetic field H_o is parallel to the cylinder axis. The length of the cylinder is assumed to be very large in comparison to R so that demagnetization effects can be neglected. We make the assumption that $d \leq 2\xi$, where ξ is the temperature-dependent ($t \equiv T/T_c$) coherence length, $\xi(t)$. The latter assumption implies that the modulus of the order parameter $F(r)$ is approximately independent of the spatial coordinate r. We make no restriction concerning the value of d in comparison to the temperature-dependent Ginzburg-Landau (GL) penetration depth $\lambda(t) \equiv \lambda$. We permit

an arbitrary number of fluxoids to be locked-in in the cylinder, the number of which is denoted by b. Because $d \leq 2\xi$ and λ is arbitrary, the solutions found in this work are valid for GL κ values $\kappa(t) < 2\lambda/d$.

In cylindrical coordinates (r, θ, z), with the applied field parallel to the z direction, the order parameter, the Gibbs free energy, and the Ginzburg-Landau equations are as follows:

$$\psi = F(r)e^{-ib\theta} , \qquad (1)$$

$$\Delta G = \frac{4}{R^2 - R_o^2} \int_0^R \left[-F^2 + \frac{1}{2}F^4 + \frac{1}{2}[h(r) - h_o]^2 \right.$$
$$\left. + \frac{1}{\kappa^2}\left[\frac{dF}{dr}\right]^2 + F^2 Q^2 \right] r \, dr , \qquad (2)$$

$$\xi^2 \frac{1}{r}\frac{d}{dr}\left[r \, \frac{dF}{dr}\right] = (F^2 + Q^2 - 1)F , \qquad (3)$$

$$\lambda^2\left[\frac{1}{r}\frac{d}{dr}\left[r\frac{dQ}{dr}\right] - \frac{Q}{r^2}\right] = F^2 Q = -\frac{4\pi}{c}\frac{2\pi\xi\lambda^2}{\phi_o}j . \qquad (4)$$

The value of b in Eq. (1) must be an integer for ψ to be single valued.

In Eqs. (2) to (4) we define:

$$\Delta G = (G_s - G_n)/(VH_c^2/8\pi) \equiv 2g ,$$

$$H_c = H_c(t) = H_c(0)(1 - t^2) \text{ and } t = T/T_c$$

(T_c measured at zero field);

$$V = \pi L(R^2 - R_o^2)$$

is the volume of the cylinder excluding the hole and

$$h(r) = H(r)/H_c(t) .$$

where $H(r)$ is the local magnetic field and $H_c(t)$ is the temperature-dependent thermodynamic critical field.

Also,

$$h_o = H_o/H_c(t) ,$$

$$Q = Q_\theta(r) = \xi[2\pi(\vec{A} \, \phi_o) + \nabla\Phi]_\theta ,$$

where the phase of the order parameter $\Phi = -b\theta$ in our case, A_θ is the vector potential, the fluxoid quantum $\phi_o = hc/2e = 2\pi\lambda\xi\sqrt{2}H_c$ and $j = j_\theta(r)$ is the supercurrent density.

For Q we write

$$Q = \frac{\xi}{r}\left[\frac{\pi r^2 H_o}{\phi_o} + \frac{\pi R^2 H_c}{\phi_o}\varphi(r) - b\right] , \qquad (5)$$

where the first term in the parentheses is proportional to the vector potential arising from the applied magnetic field. The second term is the contribution of the persistent supercurrents to the vector potential. Here $\varphi(r)$ is as yet an unknown function which will

be determined below and b is the fluxoid quantum number which must be an integer.

Interpreting Eq. (4) in terms of one of Maxwell's equations the local magnetic field $H(r)$ is

$$H(r) = \lambda\sqrt{2}H_c \vec{\nabla} \times \vec{Q} = H_o + H_c R^2\frac{1}{2r}\frac{d\varphi}{dr} . \qquad (6)$$

For $r < R_o$ the values of $F(r)$ and $H(r)$ are: $F(r) = 0$ and $H(r) = H(0)$. The boundary condition at $r = R_o$ is $H(R_o) = H(0)$, where $H(0)$ is uniform over the volume of the hole because the cylinder is assumed to be infinitely long. The function $\varphi(r)$ for $0 < r \leq R_o$ is

$$\varphi(r) = [h(0) - h_o](r/R)^2 , \qquad (7)$$

where $h(0) \equiv H(0)/H_c(t)$.

The magnetization per unit volume of the hollow cylinder, $4\pi M(t)$ is defined by

$$\frac{4\pi M(t)}{H_c(t)} = \frac{2}{R^2}\int_0^R [h(r) - h_o]r \, dr = \varphi(R) . \qquad (8)$$

where Eq. (6) was substituted into the integral and the boundary condition $\varphi(r = 0) = 0$ was applied. The magnetization per unit length of the cylinder is then $(4\pi M)(\pi R^2)$.

As mentioned above, we assume that $d < 2\xi$ so that $F(r) \equiv f \simeq \text{const.}$ bracketed by $1 \geq f > 0$. f is nonzero over the interval $R_o \leq r \leq R$ while Q, Eq. (5), is determined everywhere by taking the appropriate value of $\varphi(r)$. Substituting f into Eq. (4) and defining $x \equiv fr/\lambda$; $x_o \equiv fR_o/\lambda$; $x_1 \equiv fR/\lambda$, the solution of Eq. (4) over the interval $x_o \leq x \leq x_1$ is

$$Q(x) = AI_1(x) + BK_1(x) . \qquad (9)$$

A and B are constants of integration, and $I_1(x)$ and $K_1(x)$ are modified Bessel functions of the first kind. A and B are determined below from the boundary conditions at R_o and R. Eq. (9) must be equal to Eq. (5) over the interval $x_o \leq x \leq x_1$.

Substituting $Q(x)$, Eq. (9), into Eq. (6) one obtains over the interval $x_o \leq x \leq x_1$ the magnetic field

$$h(x) = \sqrt{2}f[AI_0(x) - BK_0(x)] . \qquad (10)$$

When x_o is substituted into Eq. (9) and Eq. (9) is equated to Eq. (5) with $\varphi(r)$ given by Eq. (7), one obtains

$$Q(x_o) = AI_1(x_o) + BK_1(x_o)$$
$$= [h(0)x_o/2\sqrt{2}f] - (fb/\kappa x_o) . \qquad (11)$$

Eliminating $h(0) = h(x_o)$ by substituting Eq. (10) into Eq. (11) leads to

$$AI_2(x_o) - BK_2(x_o) = (2fb)/(\kappa x_o^2) . \qquad (12)$$

Furthermore, at $r = R$ we have

$$h(x_1) = h_o = \sqrt{2}f[AI_0(x_1) - BK_0(x_1)] . \qquad (13)$$

Solving Eqs. (12) and (13) for the constants of integration, one obtains

$$\sqrt{2}fA = h_o[K_2(x_o) - \alpha K_0(x_1)]/\Delta \quad ,\tag{14}$$

$$\sqrt{2}fB = h_o[I_2(x_o) - \alpha I_0(x_1)]/\Delta \quad ,\tag{15}$$

with

$$\Delta = I_0(x_1)K_2(x_o) - K_0(x_1)I_2(x_o) \quad ,\tag{16}$$

$$\alpha h_o = 2\sqrt{2}(b/\kappa)(\lambda/R_o)^2 \equiv p \quad .\tag{17}$$

A and B are functions of R/λ, R_o/λ, h_o, b/κ, and f. R/λ, R_o/λ, and h_o are parameters over which an experimentalist has control, and b refers to a particular fluxoid quantum state of the cylinder. Within the present theory the values of b and κ occur always in the combination b/κ. Since, however, the value of f is unknown at this point, $A(f)$, $B(f)$, and Δ are to this extent still undetermined.

In solving Eq. (4) with $f = $ const we found that $Q = Q(fr/\lambda)$. We, therefore, cannot solve readily Eq. (3) for f since $\nabla^2 f$ is unknown; while it is most likely very small, it cannot be exactly zero since then the equation $Q^2(r) = f^2 - 1 \cong $ const would lead to a contradiction. Hence, we disregard Eq. (3) and find the value of f from the Gibbs function Eq. (2) as follows. We substitute $Q(x)$ and $h(x)$, Eqs. (9) and (10), into Eq. (2), let $F = f$ and disregard the term df/dr, keeping in mind that the constants of integration of $Q(x)$ and $h(x)$ are functions of f. Integrating Eq. (2) from $r = 0$ to $r = R$ with $f = 0$ over the interval $0 \leq r < R_o$, the result is

$$\Delta G = 2(-f^2 + \tfrac{1}{2}f^4) + h_o^2\{(a^2I_{01}I_{21} - 2acI_{01}K_{21} + c^2K_{01}K_{21})$$

$$+ s[a^2(I_{00} - 2I_{01})I_{20} + c^2(K_{00} - 2K_{01})K_{20} - 2ac(K_{00}I_{20} - K_{01}I_{20} - I_{01}K_{20})]\}/(1-s) \quad .\tag{18}$$

The following definitions are used in Eq. (18): $s = R_o^2/R^2$; $I_{01} \equiv I_0(x_1)$; $I_{21} \equiv I_2(x_1)$; $K_{21} \equiv K_2(x_1)$, etc., and $h_oa = \sqrt{2}fA$; $h_oc = \sqrt{2}fB$, where the constants of integration $A(f)$ and $B(f)$ are given by Eqs. (14) and (15).

After recasting Eq. (18) into a more convenient form for numerical computation, the extrema of ΔG with respect to f were found for constant values of h_o, R/λ, R_o/λ, and b/κ by varying f between zero and unity, or what is equivalent, from

$$\left.\frac{\partial \Delta G}{\partial f}\right|_{h_o(t),R/\lambda(t),b/\kappa(t),s} = 0 \quad .\tag{19}$$

At the extrema of ΔG the values of f were recorded and substituted into $A(f)$, $B(f)$, $Q(fr/\lambda)$, giving $h(fr/\lambda)$ and $\Delta G(f)$ as final results from our computation.

For $0 \leq r \leq R_o$ the function $\varphi(r)$ is calculated from Eq. (7) with $h(0) = h(x_o)$, where $h(x_o)$ is obtained from Eq. (10) with the appropriate value of f. For $R_o \leq r \leq R$ the function $\varphi(r)$ is obtained by equating Eqs. (5) and (9) with the appropriate f values obtained from Eq. (19). $\varphi(r)$ and $d\varphi(r)/dr$ are continuous at $r = R_o$ [see Eqs. (6) and (7)].

A quantity which is directly measurable is the magnetization. The magnetization per unit volume of the cylinder, Eq. (8), is obtained by equating Eqs. (5) and (9) at the surface of the cylinder

$$Q(x_1) = AI_1(x_1) + BK_1(x_1)$$

$$= x_1[h_o + \varphi(R)]/(2\sqrt{2}f) - fb/(\kappa x_1) \quad .\tag{20}$$

Using Eq. (13) to eliminate h_o and Eq. (12) for fb/κ

in Eq. (20) one solves for $\varphi(R)$ and obtains

$$4\pi M/H_c = \varphi(R) = h_o[cK_{21} - aI_{21} + s(aI_{20} - cK_{20})] \quad ,\tag{21}$$

where K_{21}, c, a, etc., are defined just below Eq. (18).

In the following sections we shall investigate the above theory first in the limit when $f^2 \ll 1$, in particular when H_o is kept constant and the temperature is varied. Then we shall discuss the numerical results of this theory for the general case.

Particular attention will be paid to ΔG, f, $4\pi M$, and $H(0)$ for constant values of b.

III. LIMIT OF $f^2 \ll 1$.

We now turn our attention to the second-order phase transition and supercooling phase boundaries between the normal and superconducting states of hollow cylinders for constant fluxoid quantum numbers b.

By definition, when b is constant, the critical field associated with a second-order phase transition is denoted by $H_{so}(t,b)$ and that identified with the supercooling limit by $H_{sc}(t,b)$. Both fields are obtained in the limit that $f^2 \to 0$, thus $\Delta G \to 0$. The former corresponds to a stable minimum in the Gibbs function while the latter is an unstable maximum. The dividing point between these fields is defined as the Landau critical point (LCP) where the Gibbs function has a saddle point in the limit that $f^2 \to 0$.
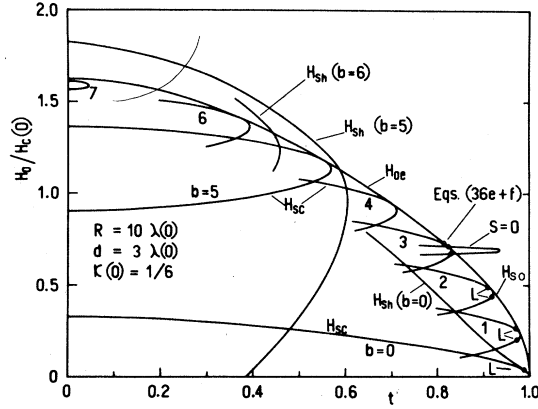
It should be emphasized that the fields as defined

FIG. 1. Shown are the phase boundaries for $f^2 \to 0$, Eq. (26'), for various fluxoid quantum numbers b, denoted by H_{sc} or H_{so}. Landau critical points, denoted by L, exist for $|b| < 4$. For temperatures $t < t_L$ the phase boundary for $b = $ const is the supercooling field H_{sc}; for $t > t_L$ it is the second-order phase-transition field H_{so}. For $|b| \geq 4$ Eq. (26') corresponds to $H_o = H_{sc}$ only. Also shown is the superheating field H_{sh} for $b = 0$, 5, and 6 discussed in Secs. III G and IV. The intersection point of Eqs. (26') and (42) ($S = 0$) determines the LCP. The envelope field, Eq. (27), is also shown as well as the LCP of a slab of thickness $d/\lambda(0) = 3$, Eqs. (46) and (47). At temperatures larger than that of the LCP the field of the slab is of second order.

here are not necessarily those of the phase boundary between the normal and superconducting states unless b is adjusted in such a way that this condition is met. This will become apparent when discussing Fig. 1 in detail.

A. $H_{so}(t,b)$ and $H_{sc}(t,b)$ for a hollow cylinder

When $0 < f \ll 1$, the Gibbs function, Eq. (18), can be expanded in a series of the following form:

$$\Delta G = P f^2 + S f^4 + U f^6 + \cdots , \qquad (22)$$

where

$$P = \frac{1}{8}\left(\frac{R}{\lambda}\right)^2 \left[h_o^2(1+s) - 4h_o ps - \frac{2(ps)^2 \ln s}{1-s}\right] - 2 , \qquad (22a)$$

$$S = \frac{1}{8}\left(\frac{R}{\lambda}\right)^4 \left[\frac{1}{4}h_o ps\left(3 - s + \frac{2s^2}{1-s}\ln s\right)\right.$$
$$\left. - \frac{1}{6}h_o^2(1 + s - 2s^2)\right.$$
$$\left. - (ps)^2\left(1 + \frac{s \ln s}{1-s}\right)\right] + 1 , \qquad (22b)$$

with

$$h_o = [H_o/H_c(0)](1 - t^2)^{-1} , \qquad (22c)$$

$$(R/\lambda)^2 = [R/\lambda(0)]^2(1 - t^4) , \qquad (22d)$$

$$ps = 2\sqrt{2}[b/\kappa(0)][\lambda(0)/R]^2(1 - t^2)^{-1} . \qquad (22e)$$

$$s = (R_o/R)^2 . \qquad (22f)$$

$$\kappa = \kappa(0)/(1 + t^2) = \lambda(t)/\xi(t) . \qquad (22g)$$

The temperature dependence of κ is chosen so as to be consistent with the definition of the fluxoid and the empirical behavior of $H_c(t)$ and $\lambda(t)$.

Since Eq. (18) is not yet minimized (or maximized) with respect to f, Eq. (22) is not minimized either. The extremum of ΔG, in the limit of $f^2 \ll 1$, is obtained from

$$\frac{d\Delta G}{df^2} = P + 2Sf^2 + 3Uf^4 + \cdots = 0 , \qquad (23)$$

with ΔG being a minimum if

$$\frac{d^2\Delta G}{(df^2)^2} = 2S + 6Uf^2 + \cdots > 0 . \qquad (24)$$

In the limit when $f^2 \to 0$, that is when we are concerned with the second-order phase-transition field H_{so} or the supercooling field H_{sc}, it follows from Eq. (23) that the equation

$$P = 0 \qquad (25)$$

is the condition which determines H_{so} or H_{sc}. Solving Eqs. (22a) with $P = 0$ leads to ($h_o \equiv h_{so}$ or h_{sc})

$$h_o = \frac{2}{(1+s)}\left\{ps \pm \left[(1+s)^2\left(\frac{2\lambda}{R}\right)^2 + (ps)^2 g(s)\right]^{1/2}\right\} , \qquad (26)$$

where

$$g(s) \equiv 1 + [(1+s)\ln s]/[2(1-s)] < 0$$

for $0 < s < 1$. Within our approximation of constant order parameter the value of the fluxoid quantum number b must be zero when $s \to 0$. This is the only possible solution in this limit.

At the magnetic field h_o, determined by Eq. (26), $f^2 \to 0$. Therefore, at this field $d^2\Delta G/(df^2)^2 = 2S$. Depending on whether $S > 0$ or $S < 0$ this field is the stable second-order phase transition field h_{so} or the unstable supercooling field h_{sc}.

In terms of temperatures ($t \equiv T/T_c$) Eq. (26) becomes

$$\frac{H_o}{H_c(0)} = \frac{4}{1+s}\left(\frac{\lambda(0)}{R}\right)^2$$
$$\times \left\{\frac{\sqrt{2}b}{\kappa(0)} \pm \left[(1+s)^2\left(\frac{R}{\lambda(0)}\right)^2\frac{1-t^2}{1+t^2}\right.\right.$$
$$\left.\left. + \left(\frac{\sqrt{2}b}{\kappa(0)}\right)^2 g(s)\right]^{1/2}\right\} . \qquad (26')$$

Equation (26') is plotted in Fig. 1 for $R/\lambda(0) = 10$, $d/\lambda(0) = 3$, $\kappa(0) = \frac{1}{6}$ for various fluxoid quantum numbers b. All our equations contain the ratio $b/\kappa(0)$ only, not b and $\kappa(0)$ separately. Thus the curve for $b = 1$ and $\kappa(0) = \frac{1}{6}$ is exactly the same as for the case $b = 4$ and $\kappa(0) = \frac{2}{3}$.

The envelope enclosing all the curves with various values of b is calculated from $P(h_o,t,b) = 0$ and $\partial P(h_o,t,b)/\partial b = 0$. After eliminating b from these two equations we obtain the equation for the field of the envelope H_{oe}:

$$\frac{H_{oe}}{H_c(0)} = \frac{4\lambda(0)}{R}\left[\frac{\ln s}{2(1-s)g(s)}\right]^{1/2}\left[\frac{1-t^2}{1+t^2}\right]^{1/2} . \quad (27)$$

This equation is valid up to a $[b/\kappa(0)]$ value given by

$$\frac{b}{\kappa(0)} = \left[\frac{R}{\lambda(0)}\right]\left[\frac{-(1+s)}{2g(s)[1-g(s)]}\right] .$$

In the limit that the wall thickness, $d \ll R$, Eq. (27) reduces to the equation for H_{so} or H_{sc} of a film in a parallel field ($H_{oe} \equiv H_{so}$ or H_{sc})

$$\frac{H_{oe}}{H_c(0)} = \sqrt{24}\frac{\lambda(0)}{d}\left[\frac{1-t^2}{1+t^2}\right]^{1/2}\left[1 - \frac{1}{120}\left[\frac{d}{R}\right]^2\right] . \quad (28)$$

Equation (27) is also shown in Fig. 1.

Furthermore, the magnetic field at the largest temperature H_{om} for a constant value of b is obtained from Eq. (26') by equating the square root in Eq. (26') to zero, solving for $(2b)^{1/2}/\kappa(0)$ and substituting this value back into Eq. (26'). This leads to

$$\frac{H_{om}}{H_c(0)} = 4\left[\frac{\lambda(0)}{R}\right]\left[\frac{-1}{(1+s)g(s)}\right]^{1/2}\left[\frac{1-t_m^2}{1+t_m^2}\right]^{1/2} . \quad (26'')$$

The value of t_m in Eq. (26'') is then the largest temperature for b_m equal to a constant. Comparing H_{om} to the field H_{oe} of the envelope at the same temperature we find

$$H_{om}/H_{oe} = [(1 - g(s)]^{-1/2} . \quad (29)$$

In the limit that $s \to 1$, Eq. (29) shows that $H_{om} \to H_{oe}$, that is, the envelope and the maximum field for constant b become identical at the same temperature and obey Eq. (28), that of a film. It is also interesting to note that H_{om}/H_{oe} is fairly insensitive to s, that is, for $0.18 < s < 1$ we have $0.9 < H_{om}/H_{oe} < 1$. In the limit that $d \ll R$, Eq. (26'') becomes

$$\frac{H_{om}}{H_c(0)} = \sqrt{24}\frac{\lambda(0)}{d}\left[\frac{1-t_m^2}{1+t_m^2}\right]^{1/2}\left[1 - \frac{7}{40}\left[\frac{d}{R}\right]^2\right] . \quad (26''')$$

Equation (26''') is again the film limit.

B. Fluxoid quantum number at the maximum temperature

If at a constant magnetic field H_{om}, corresponding to that of Eq. (26''), the temperature is swept from above T_c, then when reaching the phase boundary at $t = t_m$ a transition from the normal to the superconducting state must occur. Then the cylinder must adopt a certain fluxoid state of quantum number b_m. This b value is calculated by putting the square root equal to zero in Eq. (26'). The result for $s \neq 0$ is

$$b_m = \frac{R}{\xi(t_m)}\left[\frac{-1-s}{2g(s)}\right]^{1/2} , \quad (30)$$

where

$$\xi(t_m) = \xi(0)[(1+t_m^2)/(1-t_m^2)]^{1/2} .$$

In the limit that $d \ll R$, Eq. (30) becomes

$$b_m = \sqrt{3}\frac{R}{d}\frac{R}{\xi(t_m)}\left[1 - \frac{d}{R} + \frac{13}{40}\left[\frac{d}{R}\right]^2\right] , \quad (30')$$

where the next-higher-order term in the bracket of Eq. (30') is of order $(d/R)^4$.

C. Field and temperature spacings

1. Field spacing of phase boundaries at maximum temperatures for different b values

Consider Fig. 2 and Eq. (26'). The spacing of the magnetic fields, defined by the maximum temperature of a phase boundary for b equal to a constant, between two adjacent phase boundaries b_m and b_n with $n - m = 1$ is

$$A \equiv \frac{[H_o(t_n,b_n) - H_o(t_m,b_m)]}{H_c(0)}$$

$$= \frac{4\sqrt{2}}{1+s}\left[\frac{\lambda(0)}{R}\right]^2\frac{1}{\kappa(0)} = \frac{2}{1+s}\frac{\phi_o}{\pi R^2 H_c(0)} . \quad (31)$$

A is independent of b, t, and H_o, and is a constant for a specimen of fixed geometry. It depends only on R_o and R. ϕ_o is the fluxoid quantum. The temperature at which two phase boundaries intersect is denoted by t_x. The lower branch of the b_n phase boundary between t_x and t_n gives rise to paramagnetic magnetization, as we shall see below, while the upper branch of the b_m phase boundary gives rise to diamagnetic magnetization between t_x and t_m.

B_m/A is the ratio of the field ranges of paramagnetism to the sum of paramagnetism and diamagnetism, or in other words, B_m/A is the probability of finding a paramagnetic transition when some arbitrary magnet-
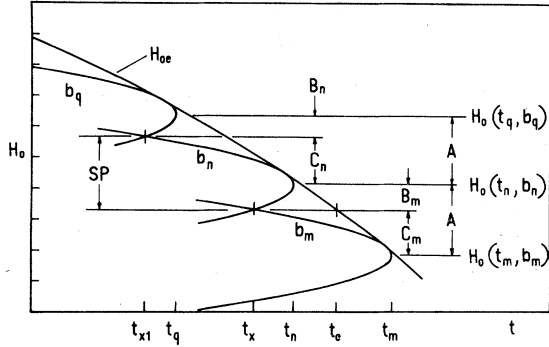
FIG. 2. Schematic plot of three phase boundaries, Eq. (26'), as a function of temperature for different fluxoid quantum numbers b and notations used with reference to Eqs. (31) to (34) and others in the text.

ic field is held constant and the temperature is swept from above T_c. From Eq. (26') one obtains a relation for t_x in terms of b_m and b_n, namely

$$H_o(t_x, b_m) = H_o(t_x, b_n) \quad .$$

When this equation is solved for t_x and substituted into

$$B_m/A = W(t_x, b_n)/[\sqrt{2}(b_n - b_m)/\kappa(0)] \quad ,$$

where $W(t_x, b_n)$ is the square root in Eq. (26') with $t = t_x$, one obtains

$$B_m/A = \tfrac{1}{2}[1 + g(s)(b_n + b_m)/(b_n - b_m)] \quad . \quad (32)$$

In the limit that $d \ll R$ and $n - m = 1$, Eq. (32), with the help of Eq. (30'), reduces to

$$2B_m/A = 1 - (2/\sqrt{3})[d/\xi(t_m)]$$

$$\times [1 + \tfrac{7}{40}(d/R)^2] - \tfrac{1}{3}(d/R)^2 \quad . \quad (32')$$

2. Field spacing between crossover temperatures t_x

Assuming that $n - m = 1$, it follows from Fig. 2 and Eq. (31) that $A = B_m + C_m = B_n + C_n$ for a specimen of fixed values R_o and R. The field spacing S between the crossover temperatures t_x and t_{x1} is then from Eq. (32) and $A = B_n + C_n$:

$$S = B_m + C_n = \tfrac{1}{2}A[2 + g(s)(2b_m + 1 - 2b_n - 1)]$$

$$= A[1 - g(s)] \quad . \quad (32'')$$

Like A, S depends only on R_o and R and is a constant for a fixed geometry. Since $g(s) < 0$, the value of S is in general larger than A, approaching the value of A for $d/R \to 0$, given by the equation ($\epsilon = d/R$)

$$S = A[1 + \tfrac{1}{3}\epsilon^2(1 + \epsilon + \tfrac{17}{20}\epsilon^2)] \quad . \quad (32''')$$

3. Temperature spacing between the envelope and crossover temperature

The temperature difference $(t_e - t_x)$ (see Fig. 2) can be calculated implicitly via the temperature dependence of the coherence lengths $\xi(t)$ at these temperatures. Substituting for $t = t_e$ into Eq. (27) and for $t = t_x$ into Eq. (26') and solving the equations $H_o(t_x, b_m) = H_{oe}(t_e) = H_o(t_x, b_n)$ with $n - m = 1$ one obtains

$$[R/\xi(t_x)]^2 - [R/\xi(t_e)]^2 = [1 - g(s)]/[2(1 + s)] \quad , \quad (33)$$

$$[\xi(t_e)/\xi(t_x)]^2 = 1 - 1/[(2b_m + 1)^2 g(s)] \quad . \quad (34)$$

The relations between b_m, t_x, and t_e are shown and defined in Fig. 2. Since $[\xi(0)/\xi(t)]^2 = (1 - t^2)/(1 + t^2)$, Eqs. (33) and (34) are the general solutions for t_e, t_x, and thus $(t_e - t_x)$. If both t_e and t_x are sufficiently close to unity, the left-hand side of Eq. (33) reduces to $(t_e - t_x)[R/\xi(0)]^2$.

In the limit that $\epsilon = d/R \ll 1$, Eqs. (33) and (34) become

$$[R/\xi(t_x)]^2 - [R/\xi(t_e)]^2 = \tfrac{1}{4}(1 + \epsilon + \tfrac{5}{6}\epsilon^2) \quad , \quad (33')$$

$$[\epsilon(t_e)/\xi(t_x)]^2 = 1 + 3/[(2b_m + 1)^2\epsilon^2(1 + \epsilon + \tfrac{17}{20}\epsilon^2)] \quad . \quad (34')$$

Therefore, when t_e and t_x are close to unity and $d/R \ll 1$ the temperature difference between the envelope and the intersection point of the phase boundaries with adjacent quantum numbers is a constant for a cylinder given by

$$t_e - t_x = (1 + \epsilon + \tfrac{5}{6}\epsilon^2)[\xi(0)/2R]^2 \quad . \quad (33'')$$

D. Superfluid velocity $Q(R)$ for $f^2 \to 0$

When $f^2 \to 0$ the critical field is either H_{so} or H_{sc} while the magnetization $4\pi M$ approaches zero. It then follows from Eq. (5) or from the fluxoid quantization relation

$$b\phi_o = \mu \int \int \vec{H} \cdot d\vec{s} + \frac{4\pi}{c}\lambda^2(t) \oint \frac{1}{F^2}[\vec{j} \cdot d\vec{l}] \quad , \quad (35)$$

evaluated at $r = R$ with

$$(4\pi/c)(\vec{j}/F^2) = -(\vec{Q}\phi_o)/[2\pi\xi(t)\lambda^2(t)]$$

[from Eq. (4)], $\mu = 1$ and $\varphi(R) = 4\pi M/H_c(t) = 0$

that ($H_o \equiv H_{so}$ or H_{sc})

$$\frac{H_o}{H_c(0)} = 2\sqrt{2}\left[\frac{\lambda(0)}{R}\right]^2 \left[\frac{b}{\kappa(0)} + \frac{R}{\lambda(0)}Q(R)\left[\frac{1-t^2}{1+t^2}\right]^{1/2}\right] . \tag{36}$$

When Eq. (36) is equated to Eq. (26′) the value of $Q(R)$ for $f^2 \to 0$ is obtained. With the help of Eq. (30) the result is

$$Q(R) = \frac{1}{u(s)}\frac{1-s}{[2(1+s)]^{1/2}}\frac{\xi(t)}{\xi(t_m)}\left\{1 \pm \frac{2u(s)}{1-s}\left[\left[\frac{\xi(t_m)}{\xi(t)}\right]^2 - 1\right]^{1/2}\right\} , \tag{37}$$

with $u(s) \equiv [-g(s)]^{1/2}$.

It follows from Eq. (30) or (30′) that in the limit of $t_m \to 1$, $b_m = 0$. Therefore for $b = 0$ it follows from Eq. (37) that

$$Q(R) = [2/(1+s)]^{1/2} . \tag{38}$$

Substituting Eq. (38) into (36) with $b = 0$, one obtains ($H_o \equiv H_{so}$ or H_{sc})

$$\frac{H_o}{H_c(0)} = \frac{4}{(1+s)^{1/2}}\frac{\lambda(0)}{R}\left[\frac{1-t^2}{1+t^2}\right]^{1/2} . \tag{26''''}$$

Equation (26′′′′) is the well-known equation of the second-order phase transition and supercooling field for a solid cylinder ($s = 0$).

When the fluxoid quantum number $b_m \neq 0$, $t_m < 1$. In the limit that the wall thickness $d \ll R$, the outside radius of the cylinder, Eq. (37) becomes ($f^2 \to 0$; $\epsilon = d/R$; $t \leq t_m$)

$$Q(R) = \sqrt{3}\left(1 - \frac{1}{2}\epsilon - \frac{7}{40}\epsilon^2\right)\frac{\xi(t)}{\xi(t_m)}$$

$$\times \left\{1 \pm \frac{1}{\sqrt{3}}(1 + \epsilon + \frac{4}{5}\epsilon^2)\left[\left[\frac{\xi(t_m)}{\xi(t)}\right]^2 - 1\right]^{1/2}\right\} . \tag{39}$$

Equations (37)−(39) show that, in general, the superfluid velocity at the outer surface of the superconducting cylinder is finite while the density of the superfluid carriers, f^2, approaches zero at the supercooling and second-order phase-transition fields.

E. Landau critical point (LCP)

The value h_o of Eq. (26) is either h_{so} or h_{sc}, depending on whether the extremum of Eq. (22) for

$f^2 \to 0$ is a stable minimum $[d^2\Delta G/(df^2)^2 > 0]$ or an unstable maximum $[d^2\Delta G/(df^2)^2 < 0]$. The dividing point between h_{so} and h_{sc} is the LCP which is defined by $d^2\Delta G/(df^2)^2 = 0$, or

$$S = 0 . \tag{40}$$

Both P and S are functions of $R/\lambda(t)$, $R_o/\lambda(t)$, $b/\kappa(t)$, and $h_o(t)$. The magnetic field H_L and the temperature T_L of the LCP are found by solving Eqs. (25) and (40) simultaneously.

1. Fluxoid quantum number b = 0

For $ps = 0$, Eqs. (22a) and (22b) can be readily solved. One obtains

$$[\lambda(t_L)/R]^2 = \frac{1}{3}[1 - 2s^2/(1+s)] ,$$

$$t_L^4 = 1 - 3[\lambda(0)/R]^2[(1+s)/(1+s-2s^2)] , \tag{41}$$

$$h^2(t_L) = 16[1 - 2s^2/(1+s)]/[3(1+s)] .$$

For a solid cylinder ($s = 0$) this reduces to the well-known equation of the LCP for $b = 0$, namely $R/\lambda(t_L) = \sqrt{3}$ and $H_L/H_c(t_L) = 4/\sqrt{3}$.

2. Fluxoid quantum number b ≠ 0 (s ≠ 0)

From Eqs. (40) and (22b) one obtains the following relation:

$$H_o/H_c(0) = [\lambda(0)/R]^2\{b/[\sqrt{2}\kappa(0)]\}y(s,b/\kappa(t)) , \tag{42}$$

where the function y is

$$y = \frac{\beta(s) \pm (\beta^2(s) + 96(1+s-2s^2)\{[\kappa(t)/b]^2 - 1 - [s\ln s/(1-s)]\})^{1/2}}{(1+s-2s^2)}$$

and $\beta(s) = 3[3 - s + 2s^2\ln s/(1-s)]$. Since $S = 0$ and $P = 0$ have a simultaneous solution when $t = t_L$ and $H_o = H_L$ for constant values of $s = (R_o/R)^2$, $b/\kappa(0)$, and $R/\lambda(0)$, the intersection point of Eqs. (26′) and (42) in the

$H_o - t$ space determines the LCP.

Figure 1 shows the LCP's for $|b| < 4$. For $b \geqslant 4$ there exists no LCP in this particular case. When LCP's exist, they exist usually in pairs for constant b. The field at the high-temperature range between the two LCP's is h_{so} while the rest of the phase boundary is defined by h_{sc}. For $b \geqslant 4$ all phase boundaries are defined by h_{sc} in this particular example.

3. Slab limit

Consider Eq. (42). Let us define a reference field $H_o = H_{or}$ which is Eq. (42) with the square root equal to zero. H_{or} is temperature independent as is H_{om}, Eq. (26') without the square root. Comparing these fields one finds

$$\frac{H_{or}}{H_{om}} = \frac{3}{8} \frac{1+s}{(1-s)(1+2s)} \left[3 - s + \frac{2s^2 \ln s}{1-s} \right] , \quad (43)$$

or $\frac{9}{8} > H_{or}/H_{om} > 1$ for $0 < s < 1$. Thus in the limit that $s \to 1 (d \ll R)$, $H_{or} \to H_{om}$. In that limit the square root of Eq. (42) is

$$24 \left\{ x \left[\left[\frac{\kappa(t)}{b} \right]^2 - \frac{1}{15} x^4 + \cdots \right] \right\}^{1/2} , \quad (44)$$

where the ellipsis indicates higher-order terms in x and $x \equiv (1-s)/(1+s)$.

We are looking for a solution of the LCP located at $t = t_m = t_L$ in the limit that $d \ll R$. At this temperature expression (44) must be zero or

$$b_m/\kappa(t_L) = (15)^{1/2}(R/d)^2 . \quad (45)$$

Replacing b_m by the dominant term of Eq. (30') one finds

$$d/\lambda(t_L) = \sqrt{5} , \quad (46)$$

a relation for the LCP of a slab. Substituting t_L for t_m into Eq. (26''') and making use of Eq. (46) one finds the well-known equation for the LCP of a slab

$$H_L/H_c(t_L) = (\tfrac{24}{5})^{1/2} . \quad (47)$$

F. Temperature dependence of magnetization for constant applied field for $0 < f^2 \ll 1$

The magnetization per unit volume $(\pi R^2 L)$ of a cylinder, $4\pi M$, is calculated from Eq. (22), neglecting terms of order f^6 and smaller. The value of f^2 at the extremum $(d\Delta G/df^2 = 0)$ of ΔG is then $f^2 = -P/2S > 0$. Substituting f^2 into ΔG one finds the value of ΔG at the extremum $\Delta G = -P^2/4S$. P

and S are functions of the applied field H_o. We assume that the magnetization of the normal state is zero. The value of M is then obtained from $[\partial (G_s - G_n)/\partial H_o]_T = -M(\pi R^2 L)$ which leads to

$$\frac{4\pi M(t)}{H_c(0)} = -\frac{1}{2}(1-s)(1-t^2)f^2 \left[\frac{dP}{dh_o} + f^2 \frac{dS}{dh_o} \right] . \quad (48)$$

The functions P and S are given by Eqs. (22a) and (22b), respectively. When we are near the phase boundary for a second-order phase transition (h_{so}), $S > 0$ and $P < 0$ with $\Delta G < 0$ being a stable minimum. Near the supercooling field h_{sc}, $S < 0$ and $P > 0$ with $\Delta G > 0$ being an unstable maximum.

Figure 3 shows the behavior of $4\pi M/H_c(0)$ and f^2 near the phase boundary for fluxoid quantum number $b = 3$ for the example shown in Fig. 1. $4\pi M$ is calculated from Eq. (48) and f^2 from $-P/2S$. Near the maximum temperature t_m the magnetization up to terms of order f^2 is zero, and becomes diamagnetic near the upper and paramagnetic near the lower branch of the $H_o - t$ phase boundary.

This can be seen readily from Eq. (48) by neglecting the term in f^4. From Eq. (22a) one obtains

$$\frac{dP}{dh_o} = \left(\frac{R}{\lambda} \right)^2 \frac{1}{4} [h_o(1+s) - 2ps] .$$

Substituting into this equation for $h_o = h_{om} + \Delta h_o$ and for $h_{om} = 2ps/(1+s)$ [from Eq. (26)], one finds that dP/dh_o is proportional to Δh_o. Sweeping temperatures at constant magnetic field, it follows that for
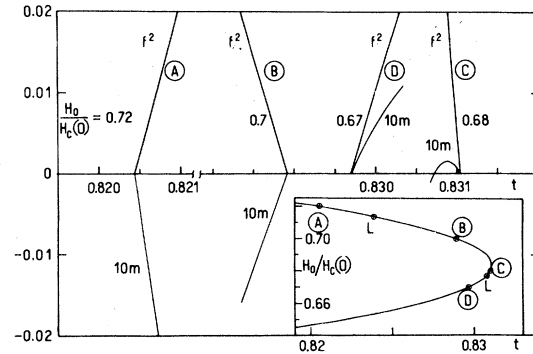

FIG. 3. Shown is the magnetization $4\pi M$ $[m = 4\pi M/H_c(0)]$ as a function of temperature for various constant magnetic fields for $b = 3$, $R/\lambda(0) = 10$, $d/\lambda(0) = 3$, and $\kappa(0) = \frac{1}{6}$ calculated from Eq. (48) and the square of the order parameter, f^2, near the phase boundary where $f^2 \ll 1$. The inset shows the applied magnetic fields with respect to the phase boundary and the Landau critical points (L). B and C are stable second-order phase transitions and A and D unstable supercooling fields. For fields $H_o/H_c(0) \geqslant 0.683$ the values of $4\pi M$ are smaller than zero near the phase boundary and for lower fields $4\pi M > 0$.

$\Delta h_o > 0$ (upper branch) $4\pi M < 0$ and for $\Delta h_o < 0$ (lower branch) $4\pi M > 0$, provided $f^2 \ll 1$ and the f^4 and smaller terms can be neglected.

When the phase boundary is defined by H_{so}, $|4\pi M|$ and f^2 increase as the temperature is decreased through the phase boundary while the energy $\Delta G = -P^2/4S$ also decreases $(S > 0)$. In this case the superconducting state is stable.

When the phase boundary is defined by H_{sc}, $|4\pi M|$ and f^2 decrease as the temperature is decreased toward the phase boundary. In this case $d^2 \Delta G/(df^2)^2 = 2S < 0$ which implies an unstable superconducting state. Therefore, in this case there must exist another superconducting state for which f^2 is not very much smaller than unity and for which the Gibbs function corresponds to a stable $(\Delta G < 0)$ or metastable $(\Delta G > 0)$ minimum.

This is shown in Fig. 4 as well as the behavior of f and $4\pi M$ for $b = 5$ for the example shown in Fig. 1. These nonlinear results will be discussed in detail in Sec. IV. The inset shows the phase boundary calculated from Eq. (26') and the contour $\Delta G = 0$ [Eq. (2)]. The superheating field H_{sh} is the field up to which solutions of the GL equations exist. Near the upper branch the unstable magnetization is diamagnetic and near the lower it is paramagnetic. Near t_m the slope of $4\pi M$ with t is zero. However, the order parameter is finite near t_m, and solutions exist for $t > t_m$. Above t_m superconducting states with energy lower than the normal state are possible.

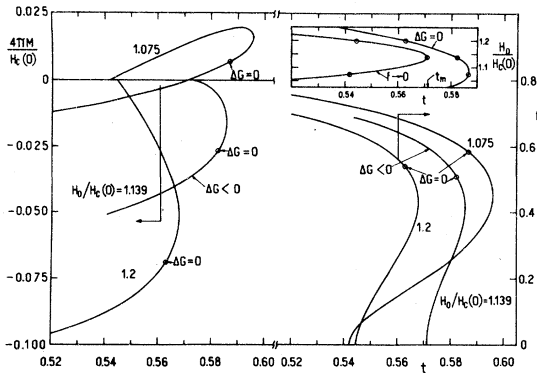It thus becomes clear, when incorporating superheating boundaries in Fig. 1, that the experimen-

tal phase boundary is not uniquely defined. This is illustrated schematically in Fig. 5 which shows that there is no unambiguous way of constructing a priori a unique phase boundary. The particular conditions under which an experiment is performed will determine which of the possible paths will be followed.

For points such as C lying between t_{sh} and t_{sc} the normal states are metastable. For a small specimen, in all likelihood, the transition from the normal to the superconducting state on lowering the temperature will take place at t_{sc}. If once in the superconducting state temperatures are again increased, either the system goes into a superconducting state with a different b value or into the normal state at some intermediate point or there is a transition to the normal state at t_{sh}.

In another experiment, starting from the normal state at R and sweeping fields at constant temperature along RS a small sample would probably become superconducting at H_{sc}. Sweeping now back towards higher fields the superconducting-to-normal transition may take place at some intermediate point, but for a small specimen it would in all likelihood occur at H_{sh}. Here also it is possible for the system to remain superconducting by changing the value of b if the radii R_o and R, and $\kappa(0)$, $\lambda(0)$, and t permit such a state.

From the above it is clear that combining field and temperature variations quite different phase boundaries may be observed experimentally as there is hysteresis in the supercooling and superheating regions.

The second-order phase boundary between the two LCP's shows reversible behavior. Combinations of both reversible and irreversible sections of the phase boundary are also possible.
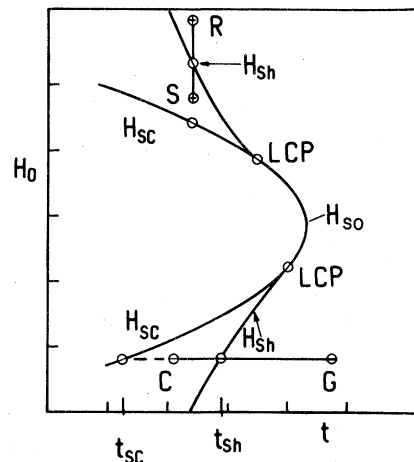

FIG. 4. Nonlinear solutions (to be discussed in detail in Sec. IV) of the magnetization $4\pi M$ and the order parameter f as a function of temperature for $b = 5$ for the sample shown in Fig. 1. The points in the inset are the locations of the applied magnetic fields on the supercooling phase boundary $(f \to 0)$ and the $\Delta G = 0$ curve shows where the Gibbs function, Eq. (2), is zero. The points where $\Delta G = 0$ are also shown on the f and $4\pi M$ curves. Note that there exist superconducting states for temperatures larger than $t_m = 1.139$ whose Gibbs free energy is smaller than that of the normal state.

FIG. 5. Schematically illustrated is the nonuniqueness of the phase boundary depending on the experiment performed. For details see text.

G. Superconducting states for temperatures $t > t_m$

When superheating is possible, there may exist quantum numbers $b > b_{min}$ for which in a constant magnetic field $H_o = H_{om}$ superconducting states are possible for temperatures $t > t_m$ and which may have an energy smaller than that of the normal state. In order to calculate b_{min} consider Figs. 1 and 6. Figure 1 shows the contours $P = 0$ (not explicitly marked) in the (H_o, t) space and one of the contours $S = 0$ (determining the LCP for $b = 3$) for a specimen of fixed values R_o, R, and $\kappa(0)$. Figure 6 shows schematically the $P = 0$ and $S = 0$ contours for $b_0 < b_1 < b_2$. Inspection of Eq. (22a) shows that the P values in the (H_o, t) space are always positive outside and always negative inside the $P = 0$ contour as indicated for the b_0 curve in Fig. 6. Similarly, it follows from Eq. (22b) that $S > 0$ inside and $S < 0$ outside the contour $S = 0$ in the (H_o, t) space.

Consider the quantum number $b_2 > b_1$ in Fig. 6. For values of $H_o = H_{om}(b_2)$ there exists, from what has been said in Sec. III F, a solution for the order parameter f in the vicinity of the $P = 0$ contour for $P > 0$ and $S < 0$, that is for $t > t_{m2}$. This solution is

$$f^2(t, h_{om}(b_2)) = -\frac{P}{2S}$$

$$= \frac{[\xi(t)/\xi(t_{m2})]^2 - 1}{[b_2/\kappa(t)]^2[w(s)/6] - 1} > 0 , \quad (49)$$

where we have substituted into P and S for $h_o = h_{om}(b_2) = 2p_2s/(1+s)$ and into P Eq. (30), that is, $[2g(s)/(1+s)]b_2^2[\xi(t_{m2})/R]^2 = -1$. $w(s)$ is pos-
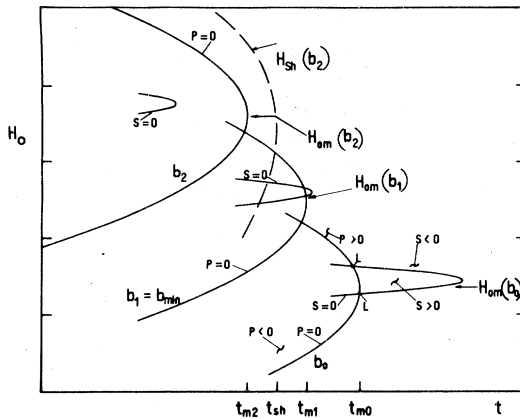

FIG. 6. Schematic relations between the $P = 0$ and $S = 0$ curves for various fluxoid quantum numbers for a given specimen. S is positive "inside" and negative "outside" the $S = 0$ curve; P is negative "inside" and positive "outside" the $P = 0$ curve. See text for b_{min} and the arguments illustrating the existence of superconducting states above t_{m2} and the nonexistence of these states above t_{m0}.

itive for $0 < s < 1$ and is defined by

$$w(s) = \left[\frac{1-s}{1+s}\right]^2 + \frac{12s}{(1+s)^2}g(s) .$$

Since for $t > t_{m2}$ the function $\xi(t)/\xi(t_{m2}) > 1$, we require that the denominator in Eq. (49) must also be larger than zero for $t > t_{m2}$ if f^2 is to be positive. This puts a restriction on the value of

$$b_2/\kappa(t) = [b_2/\kappa(t_{m2})][(1+t^2)/(1+t_{m2}^2)] ,$$

requiring that for $t > t_{m2}$ the value of $b_2/\kappa(t_{m2}) > [6/w(s)]^{1/2}$. The smallest limiting value b is obtained when

$$[b_2/\kappa(t_{m2})]^2 = 6/w(s) , \quad (50)$$

with t_{m2} defined by Eq. (30) or $(b_2 \neq 0)$

$$[b_2/\kappa(t_{m2})]^2[\lambda(t_{m2})/R]^2 = -(1+s)/[2g(s)] . \quad (51)$$

This case is shown schematically in Fig. 6 with 2 being replaced by 1;

$$b_2/\kappa(t_{m2}) \rightarrow b_1/\kappa(t_{m1}) \equiv b_{min}/\kappa[(t_m)_{max}] .$$

The solutions of Eqs. (50) and (51) then lead to the smallest quantum number b, normalized by $\kappa(0)$, and the largest temperature for which superheating for $t > t_m$ at H_{om} is no longer possible. This solution is

$$(t_m^4)_{max} = 1 + \left[\frac{\lambda(0)}{R}\right]^2 \frac{12g(s)}{(1+s)w(s)} , \quad (52)$$

$$\left[\frac{b}{\kappa(0)}\right]_{min}^2 = \frac{1}{[1+(t_m^2)_{max}]^2}\frac{6}{w(s)} , \quad (53)$$

where the s-dependent function in Eq. (52) is negative for $0 < s < 1$. For the example shown in Fig. 1 $[b/\kappa(0)]_{min} = 19.59$ or $b_{min} = 4$.

In the limit that $d \ll R$, Eqs. (52) and (53) become

$$(t_m^4)_{max} = 1 - 5[\lambda(0)/d]^2 , \quad (52')$$

$$[b/\kappa(0)]_{min} = \{\sqrt{15}/[1+(t_m^2)_{max}]\}(R/d)^2 . \quad (53')$$

It should be noted that Eqs. (52') and (53') are the same as Eqs. (45) and (46), the LCP for a slab of thickness d if $(t_m)_{max}$ is replaced by t_L. This is not too surprising when considering Eq. (26''') and the curves for $b_1 = b_{min}$ in Fig. 6.

As we have seen here, solutions for $0 < f^2 \ll 1$ are possible for $t > t_{m2}$ (see Fig. 6). These solutions, calculated from $f^2 = -P/(2S)$ are, however, unstable since they correspond to a maximum in the Gibbs function. We know, however, that the Ginzburg-Landau equations have stable solutions for $t \ll t_{m2}$ (see Fig. 5). Since these solutions must connect continuously with the unstable solutions (for $t > t_{m2}$) as

the temperature is increased at constant applied magnetic field, we must reach (for $b > b_{min}$) a superheating temperature t_{sh2} which is larger than t_{m2}.

Therefore, for $t > t_{m2}$ there must exist other solutions than those calculated from $f^2 = -P/2S > 0$ which must be stable or metastable. Some of these have been shown already in Fig. 4. These solutions are obtained below by solving the nonlinear equations numerically and are discussed there in detail.

IV. NONLINEAR SOLUTIONS OF THE GINZBURG-LANDAU EQUATIONS

This section is a summary of the results of the nonlinear solutions of the Ginzburg-Landau equations applied to a hollow cylinder with parameters $R/\lambda(0) = 10$; $d/\lambda(0) = 3$; $\kappa(0) = \frac{1}{6}$ for various fluxoid quantum numbers b. In particular solutions for $b = 0$, 3, and 5 were investigated in great detail.

Figures 1 and 4 indicate already some of the nonlinear results. Figure 1 shows the superheating boundary over part of the possible temperature ranges for $b = 0$, 5, and 6. Figure 4 exhibits the magnetization per unit volume $4\pi M$ and the order parameter near the superheating and supercooling fields as a function of temperature for various applied magnetic fields for fluxoid quantum number $b = 5$.

Figure 7 is a compilation of the superheating and supercooling fields for $t > 0.5$ for $b = 0$ to 5 with the above parameters. For these parameters the LCP's occur only when $b \leq 3$. When $b > 3$, there exist su-

perconducting states at temperatures larger than the maximum temperature of the supercooling field for a fixed value of b. This implies that for these fluxoid quantum numbers there is no second-order phase-transition region possible as discussed in Sec. III G. Therefore, in larger magnetic fields the magnetic transition from the nonmagnetic normal to the superconducting state or vice versa is that of a jump in the magnetization when the specimen is cooled or heated in a constant applied magnetic field.

At lower magnetic fields, in particular near zero magnetic field, there exist magnetic field regions, between the LCP's where the transitions are of second order. For example, in the vicinity of $H_o/H_c(0) \approx 0$, 0.23, 0.46, and 0.69 in Fig. 7. Otherwise, even in low magnetic fields, the magnetic transition corresponds to that of a jump in the magnetization. This is so in this particular case because of the choice of the parameters R, d, $\lambda(0)$, and $\kappa(0)$. As can be seen readily from Fig. 7, the LCP's exist for temperatures larger than the crossover temperature t_x (see Fig. 2) of the supercooling curves. It is possible, in particular for smaller values of b, that the LCP could be at temperatures smaller than t_x, depending on the choice of $R/\lambda(0)$, $d/\lambda(0)$, and $\kappa(0)$. This means that the phase boundary for $t > t_x$ would be of second order. For larger values of b, that is in larger magnetic fields, the LCP's have the tendency to move towards the high-temperature limit of the second-order phase-transition curve, in general, until they no longer exist in the high-field limit. The LCP's are obtained from Eq. (42) and the approximate b value corresponding to the disappearance of the LCP's is obtainable from Eq. (53). Inspection of Eq. (53) shows that the latter b value is a function of wall thickness d, outside radius R, $\lambda(0)$, and $\xi(0)$. Thus the disappearance of the second-order phase-transition region depends only on the geometrical ratios $R/\lambda(0)$, d/R, and $\lambda(0)/\xi(0)$.

The possible ambiguity of the NS phase boundary due to the superheating, supercooling, and second-order phase-transition boundaries has been discussed at the end of Sec. III F in connection with Fig. 5. It becomes clear now, by inspection of Fig. 7, that the quasiperiodic boundary between the normal and superconducting states disappears for large quantum numbers due to superheating. This disappearance was observed in large magnetic fields by Little and Parks[5] and Groff and Parks[6] on all their specimens. Even for the smaller quantum numbers, in the presence of superheating, there is a reduction of the temperature amplitude $t_e - t_x$ (see Fig. 2) of the quasiperiodic NS boundary but with t_x now being replaced by a higher temperature (see Fig. 7).

Figures 8(a)–8(d) show the order parameter f, the magnetization $4\pi M$ [Eq. (8) or (21)], the Gibbs free-energy difference ΔG [Eqs. (2) or (18) and (19)] and the magnetic field in the hole of the cylinder
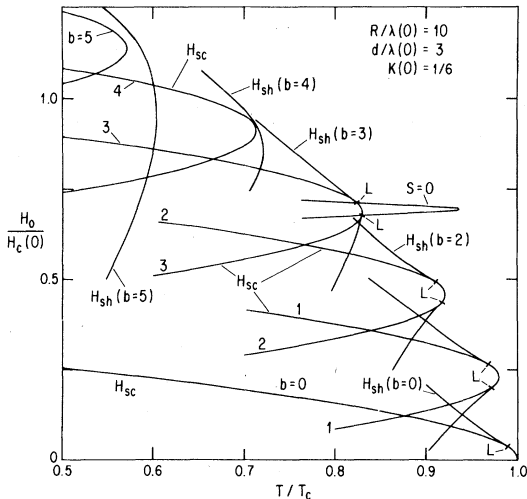

FIG. 7. Second-order phase transitions, supercooling and superheating phase boundaries for a hollow cylinder for $t > 0.5$. The fluxoid quantum numbers vary from zero to 5 and the cylinder has the following parameters: $R/\lambda(0) = 10$; $d/\lambda(0) = 3$; $\kappa(0) = \frac{1}{6}$. The Landau critical points are indicated by L.

$H(0) = H(x_o)$ [Eq. (10)] as a function of applied
magnetic field H_o for constant ambient temperatures
$t = 0.56$ and 0.58 for fluxoid quantum number $b = 5$.
The parameters are the same as in Fig. 7. Figure
8(a) shows also the f contour for $t = 0.6$. The points
on each curve in Figs. 8(a), 8(b), and 8(d) indicate
where the Gibbs free-energy difference between the
normal and superconducting states $\Delta G = 0$.

As can be seen readily from Fig. 7, there exists no
second-order phase-transition region for $b = 5$. The
maximum temperature of the supercooling boundary
$t_m = 0.5712$ (see Fig. 2 for definition) occurs at an ap-
plied field $H_o/H_c(0) = 1.139$. While for $t \lesssim t_m$ there
are superconducting states possible for $f^2 \to 0$ (un-
stable), for $t > t_m$ all the solutions correspond to
$f^2 \neq 0$, where f is not necessarily small compared to
unity but rather comparable to it. The curves for
$t = 0.56$ are typical solutions containing a supercool-
ing boundary while, for $t = 0.58$, neither supercooling
nor second-order phase-transition boundaries exist.
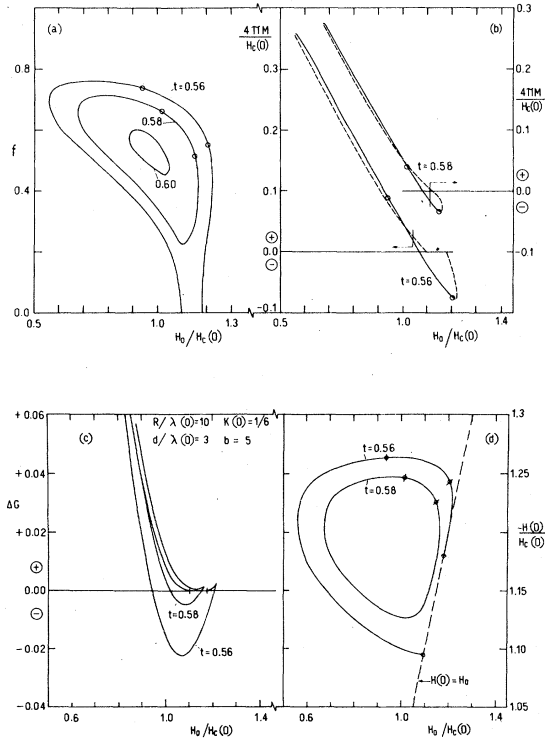As can be seen readily from Fig. 8(c), superconduct-

ing states for $t > t_m$ are not necessarily superheated
states in the sense that the Gibbs free energy of that
particular state is larger than that of the normal state,
but there exist rather extended temperature and field
regions over which $\Delta G < 0$. The upper branches in
Figs. 8(a) and 8(d) and the solid lines in Fig 8(b)
correspond to the lower branches of ΔG in Fig. 8(c);
the remaining curves correspond to the upper
branches in Fig. 8(c). The lower branch of ΔG can
be divided into two regions, a region with stable solu-
tions for which $\Delta G < 0$ and a region with metastable
solutions for which $\Delta G > 0$. The upper branch of
ΔG is always positive and corresponds to unstable
solutions.

The magnetic field in the hole of the cylinder
$H(0)$, Fig. 8(d), is always larger than the applied
field H_o in this particular case except at the super-
cooling boundary where it is equal to it. The broken
straight line is the equation $H(0) = H_o$ plotted for
comparison. Because of size effects, the magnetic
field in the hole of this cylinder is larger than $H_c(0)$.
Because $H(0) > H_o$ and Fig. 8(b) indicates that $4\pi M$
can be either positive or negative, the magnetic field
in the wall must be smaller than H_o. This was found
to be true, indeed. From Eq. (4) it follows that the
supercurrent density in the wall is proportional to
$Q(r,t)$. With a few exceptions, such as $b = 0$ and
certain limited magnetic field ranges, it was found
that the current density vanishes usually at some ra-
dius inside the wall. This implies that within the wall
of the cylinder, currents flow in opposite directions.
The point of current reversal is found to be a func-
tion of temperature and applied field even for wall
thicknesses small compared to $\lambda(0)$. The magnetic
field inside the wall is a minimum at the point where
the current density reverses direction. The magnetic
field was calculated (not shown here) at this radius,
R_c, for the case treated in Fig. 8 and found to be al-
ways less than H_o. The curves for $t = 0.56$ and 0.58
are similar to those shown in Fig. 8(d) except that
the curves are located at fields smaller than the
straight line $H(R_c) = H_o$.

To sum up the results presented in Fig. 8, we
found that, for fluxoid quantum numbers sufficiently
large, no second-order phase-transition boundary ex-
ists (no Landau critical point). For these quantum
numbers there exist stable superconducting states at
temperatures between the maximum temperature of
the supercooling boundary t_m and the maximum tem-
perature of the superheating field whose Gibbs free
energy is less than that of the normal state. The ex-
istence of such states was anticipated in Sec. III F.

Figures 9–12 show as a function of reduced tem-
perature for various constant applied magnetic fields
H_o: the order parameter f, the magnetization per
unit volume $4\pi M$, the magnetic field in the hole of
the cylinder $H(0)$, and the magnetic field within the
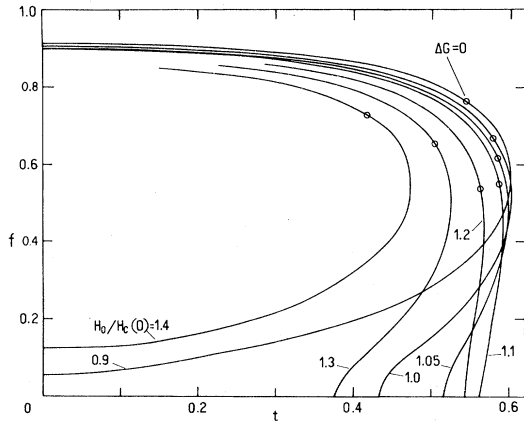wall of the cylinder $H(R_c)$ (minimum field) at the

FIG. 8. Shown are: (a) the order parameter f, (b) the
magnetization per unit volume $4\pi M$, (c) the Gibbs free-
energy difference between the superconducting and normal
states ΔG, and (d) the magnetic field in the hole of the
cylinder $H(0)$ as a function of applied field H_o for various
constant ambient temperatures. Look at (a) where the
planes of constant temperatures $t = 0.56$, 0.58, and 0.6 are
located. The cylinder parameters are: $R/\lambda(0) = 10$;
$d/\lambda(0) = 3$, $\kappa(0) = \frac{1}{6}$, and $b = 5$.

FIG. 9. Order parameter f is plotted as a function of reduced temperature $t = T/T_c$ for various constant applied magnetic fields H_o. The cylinder parameters are the same as those given in Fig. 8. The temperature dependences of $H_c(t)$, $\lambda(t)$, and $\kappa(t)$ are given by Eqs. (22c), (22d), and (22g). The circles on the curves indicate where $\Delta G = 0$. The parameters $H_o/H_c(0)$ are 0.9, 1.0, 1.05, 1.1, 1.2, 1.3, and 1.4.

point R_c at which the current density reverses direction of flow. The size and material parameters for the cylinder are $R/\lambda(0) = 10$, $d/\lambda(0) = 3$, and $\kappa(0) = \frac{1}{6}$. The fluxoid quantum number is held fixed at $b = 5$.

The larger values of f for $H_o/H_c(0) = \text{const}$, at a fixed temperature, corrrespond to stable or metastable solutions of the GL Equations. The point of metastability occurs where $\Delta G = 0$ which is indicated by a circle on the curves. For temperatures smaller than that at which $\Delta G = 0$, the solutions are stable (within the context that $b = 5$ is the only controlling quantum number), for higher temperatures they are

FIG. 11. The magnetic field in the hole of a long cylinder is shown as a function of reduced temperature for various constant applied magnetic fields. The data are the same as those used in Fig. 9 except that $H_o/H_c(0)$ is 0.9, 1.05, 1.20, and 1.30.

metastable on the upper branch and reach the limit of metastability at the temperature where solutions of the GL equation cease to exist. The lower branch is unstable. Temperatures and fields for $f \rightarrow 0$ correspond to the supercooling curve for $b = 5$ shown in Fig. 1. The curves for $H_o/H_c(0)$ equal to 1.4 and 0.9 indicate that supercooling is not possible at these fields for $b = 5$. The latter curves are somewhat similar in nature to those shown in Fig. 8 for $t = 0.58$ and 0.6.

The magnetization per unit volume $4\pi M$, shown in Fig. 10, can be either diamagnetic (negative) or paramagnetic (positive) when the applied magnetic field H_o is held constant and the temperature is changed. The sign of the magnetization will depend, for example in an experiment, to which value of the field and/or temperature one is able to lock the specimen for a given fluxoid quantum state b ($b = 5$ in
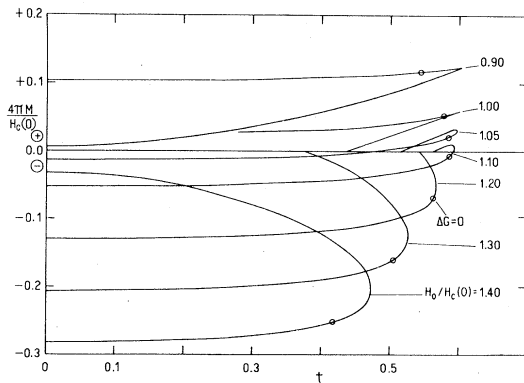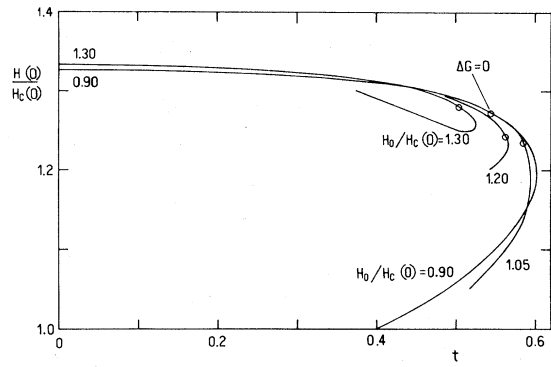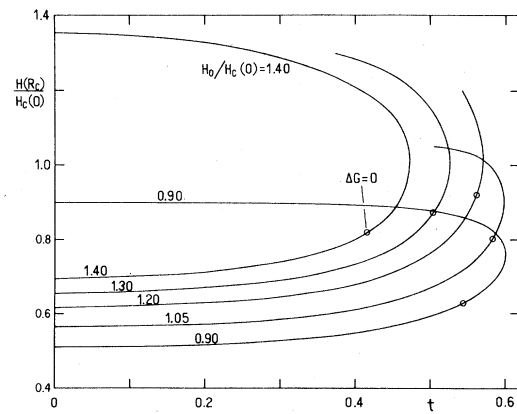

FIG. 10. Shown is the magnetization per unit volume $4\pi M$ of a hollow cylinder as a function of reduced temperature for various constant magnetic fields. The data are the same as those used in Fig. 9.

FIG. 12. Magnetic field within the wall of the cylinder $H(R_c)$ at the point R_c at which the current density is zero (supercurrent density reverses direction of flow at R_c) as a function of reduced temperature. The cylinder parameters are the same as those stated in the caption of Fig. 9.

this case). For $4\pi M < 0$, the lower branch is stable or metastable, and for $4\pi M > 0$ it is the upper branch, in general, provided one takes $t = 0$ as the reference temperature for deciding the sign of the magnetization. Thus, it is possible, within the domain in which the fluxoid quantum number b is conserved, when entering the superconducting state from the normal state by cooling the specimen in a constant magnetic field, that $4\pi M$ will be negative and reversible with temperature. Then if the field is reduced sufficiently, at lower temperatures, the specimen becomes paramagnetic [see also Fig. 8(b)]. For subsequent heating of the specimen in the latter field, the cylinder remains paramagnetic until it enters the normal state or changes the fluxoid quantum number. This behavior of the magnetization is quite different from that of the giant vortex state as found in Ref. 1. The giant vortex state corresponds to the quantized fluxoid state of the surface sheath on a solid cylinder which is much thicker than $\xi(t)$. In a sufficiently thick solid cylinder the surface sheath has the freedom to adjust its thickness to accommodate for changes in fields and temperature. However, for cylinders which we are investigating here for which $d \lesssim 2\xi$, the width of the superconducting region is determined by the wall thickness of the cylinder at all fields and temperatures within the validity of our approximations. This is the source of the different temperature behaviors.

This difference shows up also in the Gibbs free energy ΔG when plotted as a function of temperature for H_o being constant (not shown). The lower branch of ΔG is approximately parabolic with the minimum located at $t = 0$ K. The absolute minimum of ΔG occurs for $H_o/H_c(0) \simeq 1.05$ for the above cylinder with $b = 5$. Magnetic fields and temperatures where $\Delta G = 0$ are indicated in Fig. 4 and Figs. 8–12.

Figure 11 shows the magnetic field in the hole of the cylinder as a function of reduced temperature for various applied magnetic fields H_o. The upper branches are the stable ones up to temperatures at which $\Delta G = 0$. It should be noted that $H(0)$ is rather insensitive to the exact value of the applied magnetic field for $\Delta G \lesssim 0$ when the temperature is varied.

$H(0)$ is to first approximation a constant at low temperatures and its value is found to scale with b. At the supercooling field where $f^2 \to 0$, the value of $H(0) \to H_o$, the applied magnetic field.

Figure 12 is a plot of the smallest value of the magnetic field in the wall of the cylinder which occurs at the point $r = R_c$ at which the current density is zero (point of reversal of current direction). The lower branches correspond to stable solutions of the GL equations, and $H(R_c) \to H_o$ when $f^2 \to 0$. The current density does not reverse direction anywhere in the cylinder for $b = 0$, but for $b \geq 1$ there exists usually a reversal point regardless of wall thickness d

in relation to $\lambda(0)$. One finds that $H(R_c)$ is always smaller than H_o. Compared to $H(0)$ at low temperatures, the stable solution of $H(R_c)$ is considerably more sensitive to the applied magnetic field than $H(0)$.

V. COMPARISON WITH EXPERIMENTS

Here we shall make a comparison between the equations derived in Sec. III and the detailed experiments of Groff and Parks[6] which are an extension of the experiments by Little and Parks[5] and Parks and Little.[5] Furthermore, a comparison between the nonlinear results of Sec. IV and the experiments of Goodman et al. will be made.

The excellent experiments of Groff and Parks[6] show plots of the phase boundary between the normal and superconducting states similar to that shown in Figs. 1 and 7. Their Fig. 7 is a representative plot of Al hollow cylinders and their Figs. 9 and 11(c) of Sn hollow cylinders. The measured magnetic fields [not normalized by $H_c(0)$] are plotted as a function of temperature. It will be shown that from their experimental results, namely from the envelope curve, from b, t_m, t_x, and the field spacings of the temperature maxima, e.g., $\Delta H_{om} = H_o(t_n, b_n) - H_o(t_m, b_m)$ (see Fig. 2), and the field spacing between the intersection points of the "parabolas" some of the fundamental constants of the superconductors and the dimensions of the hollow cylinder can be calculated. These are R, d, R_o, $\xi(0)$, and the product $H_c(0)\lambda(0)$.

It follows from Eqs. (30) and (31) that

$$\xi(0)[-g(s)]^{1/2}\frac{1}{R}\left(\frac{2}{1+s}\right)^{1/2} = \frac{1}{b_m}\left(\frac{1-t_m^2}{1+t_m^2}\right)^{1/2} \equiv q^{-1} \ ,$$

(54)

$$\frac{1}{R}\left(\frac{2}{1+s}\right)^{1/2} = \left(\frac{\pi\Delta H_{om}}{\phi_o}\right)^{1/2} \ .$$

(55)

Since b_m, t_m, and ΔH_{om} can be readily measured, Eqs. (54) and (55) constitute two equations with the three unknowns $\xi(0)$, R, and s. If the measured $H - T$ phase boundary represents truly the second-order or supercooling phase boundary, not influenced by superheating effects, then it is probably more reliable to calculate the shape factor $g(s)$ (thus the value of s) from the temperatures t_e and t_x, that is from Eq. (34)

$$[-g(s)]^{-1} = (2b_m + 1)^2\{[\xi(t_e)/\xi(t_x)]^2 - 1\} \ ,$$

(56)

where the relations between b_m and t_e and t_x are defined in Fig. 2. A similar relation, but involving Eqs.

(54) and (33) is

$$[-g(s)]^{-1} = 4q^2 \left[\left[\frac{\xi(0)}{\xi(t_x)} \right]^2 - \left[\frac{\xi(0)}{\xi(t_e)} \right]^2 \right] - 1 \quad . \tag{57}$$

The experiments of Groff and Parks[6] are mainly second-order phase-transition boundaries as we shall see below. Thus Eqs. (56) and (57) are applicable in this case. If t_x is determined or changed by superheating effects, Eqs. (56) and (57) are no longer applicable nor is the field spacing between the intersection points at t_x given by

$$H_o(b_m, t_{x1}) - H_o(b_m, t_{x2}) = \Delta H_{om}[1 - g(s)] \quad . \tag{58}$$

In that case it is possible to obtain $g(s)$ from the scaling constant of the envelope field [Eqs. (27), (31), and (54)]:

$$H_{oe} = q \Delta H_{om}[1 - g(s)]^{1/2} \left[\frac{1 - t^2}{1 + t^2} \right]^{1/2} \quad . \tag{59}$$

However, if $|g(s)| \ll 1$, Eq. (59) is less accurate than Eq. (56).

Figure 13(a) shows the results for Al with $\Delta H_{om} = 14.0$ G, $q = 15.04$, and $g(s) = -0.042\,62$ [calculated from Eq. (56); $s = 0.4876$] leading to $\xi(0) = 2210$ Å, $R = 7950$ Å, $d = 2400$ Å, $H_{oe}(0) = 215.0$ G, and $H_c(0)\lambda(0) = 1.054 \times 10^{-3}$ G cm [from ϕ_o with $\xi(0)$]. Since Eq. (26') can also be written

$$H_o = \frac{2}{1+s} \frac{\phi_o}{\pi R^2} \left\{ b \pm \left[\left[\frac{1+s}{2} \right] \left[\frac{R}{\xi(t)} \right]^2 + b^2 g(s) \right]^{1/2} \right\} \quad ,$$

it is obvious that only b, R, d, and $\xi(0)$ are necessary to calculate H_o as a function of t; while $H_c(0)$ and $\lambda(0)$ are not. Furthermore, the above radius R is the outside radius and is not to be confused with the radius R used by Groff and Parks.[6] We denote their R value by R_{eff} which is defined by their Eq. (10), $R_{eff}^2 = R_m^2/[1 + \frac{1}{3}(d/2R_m)^2]$, where $R_m = \frac{1}{2}(R_o + R)$, the mean radius. With the above values of R and d one obtains $R_{eff} = 6720$ Å. This compares to the values given by Groff and Parks[6] as follows: $R_{eff} = 6650$ Å, $d = 2500$ Å, $H_{oe}(0) = 220$ G, and $H_c(0)\lambda(0) \simeq 1.07 \times 10^{-3}$ G cm ($T_c = 1.152$ K).

Similarly, Fig. 13(b) shows the calculations for Sn with $\Delta H_{om} = 17.7$ G, $q = 21.31$, and $g(s) = -0.056\,01$ [from Eq. (56); $s = 0.4385$] leading to $\xi(0) = 1210$ Å, $R = 7190$ Å, $d = 2430$ Å, $H_{oe}(0) = 387.2$ G, $H_c(0)\lambda(0) = 1.924 \times 10^{-3}$ G cm, and $R_{eff} \simeq 5900$ Å. This compares to the values given by Groff and Parks as follows: $R_{eff} = 6000$ Å, $d = 2500$ Å, $H_{oe}(0) = 390$ G, and $H_c(0)\lambda(0) \simeq 1.945 \times 10^{-3}$ G cm ($T_c = 3.728$ K).

In Fig. 13 are also shown the LCP's and one of the superheating boundaries (Sn; $b = 1$; upper branch). Thus superheating could not have influenced these experiments within the experimental accuracy and the

measured phase boundaries are mainly of second order over most of the temperature ranges.

Figure 14 shows experiments by Goodman et al.[11] on a hollow tin cylinder of inside radius $R_o = 70\,000$ Å and wall thickness $d = 5000$ Å. They[11] usually observed that the trapped flux of quantum state $b = 1$ decreased by about 20% before a jump to $b = 0$ occurred. The specimen shown in their Fig. 9 showed a continuous decrease by about 30% when the temperature was raised towards T_c and is shown in Fig. 14. They fit their experimental data to their Eq. (4) which is an approximation based on Eq. (35) with $F^2 = 1$ and assuming uniform current density in the cylinder wall. Their fit leads to $\lambda(0) = 1200$ Å which is by a factor of 2 too large than the usually accepted value for tin. Although our numerical results show that for the shown temperature range the magnetic field has no minimum inside the wall for $b = 1$, (at lower temperatures there is a minimum, implying that currents flow in opposite directions), the current density is not uniform. Furthermore, the order
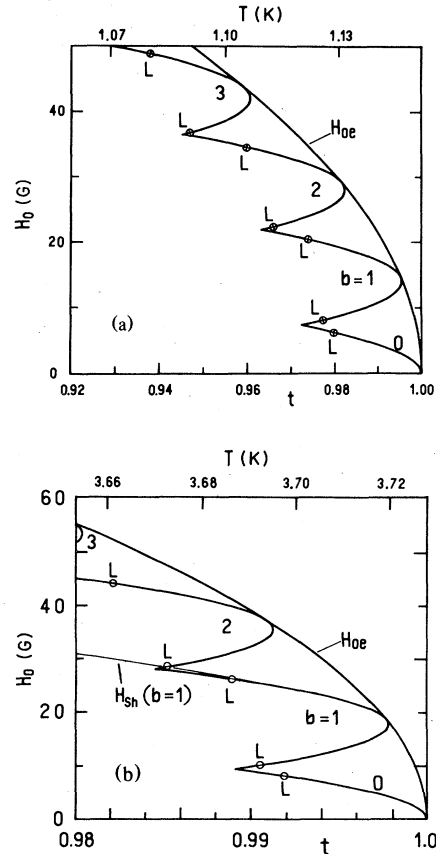

FIG. 13. (a) Calculated results for the experiments on aluminium by Groff and Parks (Ref. 6) relating to their Fig. 7. For details see text. (b) Calculated results for the experiments on tin by Groff and Parks (Ref. 6) relating to their Figs. 9 and 11(c). For details see text.
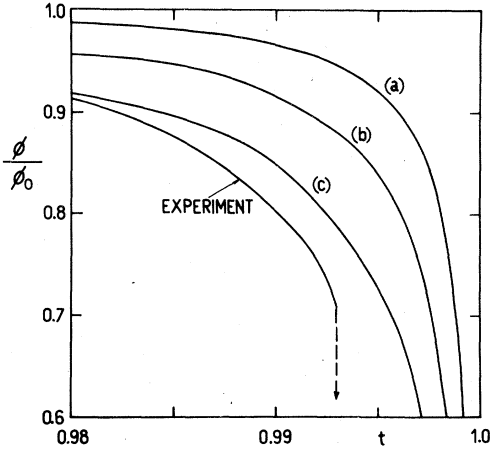
FIG. 14. Trapped flux in a hollow cylinder as a function of temperature for fluxoid quantum number $b = 1$. Experiments are by Goodman *et al.* (Ref. 11) on a tin cylinder of outside radius $R = 75\,000$ Å, wall thickness $d = 5000$ Å. Calculated curves (a) to (c) are from the nonlinear equations; all with $H_c(0) = 304.8$ G; $T_c = 3.750$ K, and $R = 75\,000$ Å. Curve (a) for $d = 5000$ Å, $\lambda(0) = 600$ Å; (b) for $d = 2500$ Å, $\lambda(0) = 600$ Å; and (c) for $d = 5000$ Å, $\lambda(0) = 1200$ Å. The quantum state of the specimen jumps to $b = 0$ when $\phi/\phi_o \simeq 0.71$.

parameter decreases near T_c as the temperature is raised towards T_c. Curves (a) to (c) are results of our numerical calculations for different values of $\lambda(0)$ and d as stated in the figure caption. It seems that curve (c) with $\lambda(0) = 1200$ Å is close to the experimental results. The trapped flux was calculated from $\phi = \pi R^2(H_o + 4\pi M)$ with $H_o = 0$.

VI. CONCLUSIONS

Solutions of the GL equations were found for a long hollow superconducting cylinder in an axial magnetic field provided the wall thickness d was smaller than $2\xi(T)$. It was found previously,[1,2] when investigating a multiply connected surface sheath on a macroscopic cylinder, that at H_{c3} the fluxoid quantum is locked in to the value $b = (1.695/2)(R/\xi)^2 - R/\xi$. Thus for $R \gg \xi$ the quantum number b at H_{c3} is determined by the total number of flux quanta applied to the cylinder $[(1.695/2)(R/\xi)^2]$ minus the number of flux quanta contained in the annular area $2\pi R\,\delta$ of the cylinder, where $\delta = 0.5901\xi$. By expanding the Gibbs function, Eq. (18), for $f \rightarrow 0$ one finds a similar relation for a hollow cylinder. This implies that when a transition from the N to the S state is made, for example by cooling in a constant magnetic field H_{om} [Eq. (26″)], that b_m [Eq. (30)] is

$$b_m = (\phi_a - H_{om}2\pi R\,\delta)/\phi_o \quad . \tag{60}$$

where the applied flux $\phi_a = \pi R^2 H_{om}$ and $\delta = \frac{1}{2}d$

$\times (1 - \frac{1}{2}d/R)$. Thus at H_{om} the flux contained in the annular area $2\pi R\,\delta$ is excluded from assigning the fluxoid quantum number. The distance δ determines the contour at which the superfluid velocity in the wall of the cylinder is zero. This contour is the reversal point of the current density inside the wall which exists always at H_{om} regardless of the value of the ratio d/R even when $d \ll \lambda(t)$.

Equation (26) is the second-order phase-transition boundary or supercooling boundary between the N and S states. For a fixed value of b it depends only on R, d, and $\xi(t)$ (see also Sec. V). The magnetic field spacing of the temperature maximum between adjacent fluxoid quantum numbers is a function of R and d only [Eq. (31)] and approaches $\phi_o/\pi R^2$ when $d \ll R$ and $2\phi_o/\pi R^2$ when $d \rightarrow R$. The field spacing between the crossover temperatures t_x depends on R and d only and is given by Eq. (32″).

Because $g(s) < 0$, it follows from Eq. (32) that B_m (see Fig. 2) can be positive or negative since $(b_n + b_m)/(b_n - b_m) = 2b_m + 1$ for $b_n - b_m = 1$. In the region where $B_m > 0$ the transition at the NS phase boundary is paramagnetic as discussed in Sec. III F. A negative B_m value means that the $H_o(t,b_m)$ curve intersects the $H_o(t,b_n)$ curve on the upper branch, meaning that $H_o(t_x,b_n) > H_o(t_n,b_n)$. This reversal of sign of B_m will depend on the fluxoid quantum number b_m for a given value of $g(s)$ and is a consequence of the fact that the spacing $\mathcal{S}$ [Eq. (32″)] is always larger than A [Eq. (31)]. In particular, when $(d/R)^2 \rightarrow 0$ the value of B_m is always negative for $d/\xi(t_m) > 0.866$ [Eq. (32′)] for all values of b. This is consistent with the surface critical field[23] $H_{c3}(b)$ as a function of $[R/\xi(t)]^2 \propto (1 - t^2)/(1 + t^2)$ where there are[23] intersection points equivalent to $B_m < 0$. As discussed in Sec. III F, the second-order phase transition at the NS phase boundary is diamagnetic when the hollow cylinder is cooled in an axial field $H_o = H_o(t,b_m) > H_o(t_m,b_m)$. Therefore, a large hollow cylinder for which $(d/R)^2 \ll 1$ and $d/\xi(t_m) > 0.866$ will always show a diamagnetic transition $(B_m < 0)$ at the NS phase boundary, regardless of the value of b, when *cooled* in a magnetic field (provided the phase transition is of second order).

It is interesting to note [from Eq. (37)] that the superfluid velocity $Q(R)$ at the surface of the cylinder depends only on the ratio d/R when $t = t_m$ and is finite when the order parameter $f \rightarrow 0$. Substituting this value of $Q(R)$ into Eq. (36) with $t = t_m$ and replacing $b = b_m$ by Eq. (30) one obtains Eq. (26″). The independence of $Q(r)$ on t_m (at $t = t_m$) is also consistent with Eq. (5) since the products $H_{om}\xi(t_m)$ and $b_m\xi(t_m)$ are independent of t_m and $\varphi(r) \rightarrow 0$ as $f \rightarrow 0$. A special case is $b = 0$ for which $Q(R)$ is a function of d/R only for all values of t [Eq. (38)] in the limit that $f \rightarrow 0$.

The envelope of the NS phase boundary is given by Eq. (27) and the temperature spacing between the

envelope and t_x for constant H_o is discussed in Sec. III C *3*.

Whether t_x is located in the second-order phase-transition region or the supercooling region will depend on the location of the Landau critical point which is the dividing point between them. The latter depends for a fixed value of b on R, d, and $\kappa(t)$ [Eq. (42) with $\phi_o = 2\pi\sqrt{2}H_c(0)\lambda(0)\xi(0)$]. If the LCP is located at a temperature smaller than t_x, then the NS phase boundary is of second order, otherwise the boundary for $t < t_{LCP}$ is in the supercooled state. In the latter case there exist also superheating boundaries in field and temperature (Fig. 5) up to which stable and metastable solutions exist besides the unstable ones (Figs. 4 and 7). For larger quantum numbers the LCP moves towards $H_o(t_m)$ and for still larger b values it ceases to exist at all (Figs. 6 and 7). In the latter case the phase boundary for constant b is solely a supercooling boundary for $f \to 0$. The superheating boundary is then partly located at temperatures above t_m, the maximum of the supercooling boundary. For $t > t_m$ stable and metastable states exist (Figs. 7–12). The latter solutions are probably distantly related to the superheated surface sheath[29–32] for $0.407 < \kappa < 0.595$. The latter solutions were derived[29,30] for the semi-infinite half-space without taking fluxoid quantization into account and exist[31,32] for $H_o < H_c(t)$. Whether the quantized superconducting surface sheath may have, under certain circumstances, superheated states possible for $H_o > H_c$, similar to our solutions (Fig. 8 for $t > t_m$) is unknown at present. The observed tails in the expelled flux of Ref. 1 could possibly have such an origin.

The magnetic field in the hole of the cylinder, $H(0)$, as a function of temperature is approximately the same for all stable solutions for most values of the applied magnetic field for b being constant (Fig. 11). $H(0)$ scales linearly with b for $t \to 0$.

The quantitative agreement between Groff and Parks's[6] measured NS phase boundary on Sn and Al and our calculated phase boundary [Eq. (26)] including the Landau critical points is excellent (Fig. 13). The agreement with the measured temperature dependence of Goodman *et al.* of the trapped flux for quantum state $b = 1$ and our numerical (nonlinear) results is only qualitative (Fig. 14). A translation of the temperature scale or a change of one of the cylinder dimensions could lead to better agreement.

ACKNOWLEDGMENTS

*Permanent address: Dept. of Electrical and Computer Engineering, Univ. of California, Davis, Calif. 95616.

†Temporary address: Dept. of Phys., Univ. of California, Davis, Calif. 95616.

[1]F. de la Cruz, H. J. Fink, and J. Luzuriaga, Phys. Rev. B 20, 1947 (1979).

[2]A. López and H. J. Fink, Phys. Lett. A 72, 173 (1979).

[3]T. K. Hunt and J. E. Mercereau, Phys. Rev. 135, A944 (1964).

[4]J. E. Mercereau and T. L. Crane, Phys. Rev. Lett. 12, 191 (1964).

[5]W. A. Little and R. D. Parks, Phys. Rev. Lett. 9, 9 (1962); R. D. Parks and W. A. Little, Phys. Rev. 133, A97 (1964).

[6]R. P. Groff and R. D. Parks, Phys. Rev. 176, 567 (1968).

[7]L. Meyers and R. Meservey, Phys. Rev. B 4, 824 (1971).

[8]N. Byers and C. N. Yang, Phys. Rev. Lett. 7, 46 (1961).

[9]B. S. Deaver, Jr., and W. M. Fairbank, Phys. Rev. Lett. 7, 43 (1961).

[10]R. Doll and M. Näbauer, Phys. Rev. Lett. 7, 51 (1961).

[11]W. L. Goodman, W. D. Willis, D. A. Vincent, and B. S. Deaver, Jr., Phys. Rev. B 4, 1530 (1971).

[12]L. Onsager, Phys. Rev. Lett. 7, 50 (1961).

[13]J. Bardeen, Phys. Rev. Lett. 7, 162 (1961).

[14]J. B. Keller and B. Zumino, Phys. Rev. Lett. 7, 164 (1961).

[15]M. Tinkham, Phys. Rev. 129, 2413 (1963).

[16]M. Tinkham, Rev. Mod. Phys. 36, 268 (1964).

[17]R. Meservey and L. Meyers, Phys. Rev. B 6, 2632 (1972).

[18]L. J. Barnes and H. J. Fink, Phys. Lett. 20, 583 (1966).

[19]L. J. Barnes and H. J. Fink, Phys. Rev. 149, 186 (1966).

[20]D. S. McLachlan, Phys. Rev. Lett. 23, 1434 (1969).

[21]H. J. Fink and A. G. Presson, Phys. Rev. 151, 219 (1966); 168, 399 (1968).

[22]J. Luzuriaga and F. de la Cruz, Solid State Commun. 25, 605 (1978).

[23]D. Saint-James, Phys. Lett. 15, 13 (1965).

[24]C. Dalmasso and E. Pagiola, Nuovo Cimento 35, 811 (1965).

[25]P. Michael and D. S. McLachlan, J. Low Temp. Phys. 14, 607 (1974).

[26]H. J. Lipkin, M. Peshkin, and L. J. Tassie, Phys. Rev. 126, 116 (1962).

[27]D. H. Douglass, Jr., Phys. Rev. 132, 513 (1963).

[28]H. J. Fink, D. S. McLachlan, and B. Rothberg-Bibby, in *Progress in Low Temperature Physics*, edited by D. F. Brewer (North-Holland, Amsterdam, 1978), Vol. VIIB, p. 435.

[29]J. Feder, Solid State Commun. 5, 299 (1967).

[30]J. G. Park, Solid State Commun. 5, 645 (1967).

[31]J. P. McEvoy, D. P. Jones, and J. G. Park, Solid State Commun. 5, 641 (1967); J. P. McEvoy, D. P. Jones, and J. G. Park, Phys. Rev. Lett. 22, 229 (1969).

[32]F. W. Smith and M. Cardona, Phys. Lett. A 25, 671 (1967).